Continuum Models for Beam- and Platelike Lattice Structures

Ahmed K. Noor,* Melvin S. Anderson,† and William H. Greene‡
NASA Langley Research Center, Hampton, Va.

A simple, rational approach is presented for developing continuum models for large repetitive beam- and platelike lattices with arbitrary configurations subjected to static, thermal, and dynamic loadings. The continuum models for these structures are shear flexible beams and plates. They account for local effects in the repeating element of the actual structure and are characterized by their thermoelastic strain and kinetic energies, from which the equations of motion and constitutive relations can be derived. The procedure for developing the expressions for thermoelastic strain and kinetic energies of the continuum involves introducing basic assumptions regarding the variation of the temperature, displacement, and strain components in one or two directions (for plate- and beamlike lattices) and obtaining effective thermoelastic and dynamic coefficients of the continuum in terms of material properties and geometry of the original lattice structure. The high accuracy of the continuum models developed is demonstrated by means of numerical examples.

Nomenclature

A_1, A_2, A_b, A_d = cross-sectional areas of members of the lattice
a_1, a_2 = side lengths of platelike lattices
a = planform area of repeating element of platelike lattice
b, d, L = length of members of the lattice
$C_{\alpha\beta\gamma\rho}, \bar{C}_{33\alpha\beta}, \bar{C}_{3333}$ = extensional stiffnesses of continuum plate model
$C_{\alpha 3\beta 3}$ = transverse shear stiffnesses of plate model
$C_{11}, C_{22} \rightarrow C_{66}$ = stiffnesses of continuum beam model
C_T, F_T, D_T = effective thermoelastic stiffnesses of continuum models
$D_{\alpha\beta\gamma\rho}$ = bending stiffnesses of plate model
E = elastic modulus of the material
$F_{\alpha\beta\gamma\rho}, F_{\alpha 3\beta\gamma}$ = stiffness interaction coefficients of plate model
h = distance between top and bottom surfaces of double-layered grids
K = kinetic energy
$\bar{L}$ = length of repeating element of beamlike lattice
$\ell_i^{(k)}$ $(i=1\rightarrow 3)$ = direction cosines of member k
$m_0, m_1, m_2, m_{02}, m_{03}, m_{23}, m_{22}, m_{33}$ = density parameters of continuum models
n = number of bays of the lattice
P_1^j, P_2^j, P_3^j = external load components in the coordinate directions at node j
$T^0, \partial_i T^0$ $(i=1\rightarrow 3)$ = uniform temperature and temperature gradients in the x_i coordinate directions
$\bar{U}, U$ = thermoelastic and isothermal strain energies
U_ℓ, U_q = contributions of linear and quadratic terms in T^0 and $\partial_i T^0$ to the strain energy
u_1, u_2, w = displacement components in coordinate directions
W = work done by external forces
x_1, x_2, x_3 = Cartesian coordinate system
$\alpha_1, \alpha_2, \alpha_b, \alpha_d, \alpha_v$ = coefficients of thermal expansion of members of lattice
ϕ_1, ϕ_2, ϕ_3 = rotation components
ω = circular frequency of vibration
ϵ_{ij} $(i,j=1\rightarrow 3)$ = strain components in coordinate directions
$\epsilon_1^0, 2\epsilon_{12}^0, 2\epsilon_{13}^0$ = extensional and transverse shear strains of beam model
$\kappa_{\alpha\beta}^0$ = curvature changes and twist of plate model
$\kappa_2^0, \kappa_3^0, \kappa_t^0$ = curvature changes and twist of beam model
$\rho_1, \rho_2, \rho_b, \rho_d, \rho_v$ = mass density of lattice members
∂_i $\equiv \partial/\partial x_i$ $(i=1\rightarrow 3)$

Received Feb. 16, 1978; presented as Paper 78-493 at the AIAA/ASME 19th Structures, Structural Dynamics, and Materials Conference, Bethesda, Md., April 3-5, 1978; revision received July 21, 1978. This paper is declared a work of the U.S. Government and therefore is in the public domain.

Index categories: Structural Dynamics; Structural Statics; Thermal Stresses.

*Professor of Engineering and Applied Science, The George Washington University Center. Associate Fellow AIAA.

†Principal Scientist, Structural Mechanics Branch, Structures and Dynamics Division. Member AIAA.

‡Graduate Research Assistant, The George Washington University Center.

Introduction

BECAUSE of increasing interest in large lattice-type structures for space applications, approximation of repetitive lattice grids with equivalent continuum models has gained popularity in recent years. Continuum models provide a simple means of comparing structural characteristics of lattices with different configurations and assessing the sensitivity of their responses to variations in material and geometric properties. Conventional finite-element analyses of such grids with a very large number of nodes are expensive and time-consuming. The continuum approximation, therefore, provides a very practical solution method for overall response and is particularly useful from the preliminary design point of view.

The key to approximation of lattice grids by continuum models is the selection of relationships between the geometric and material properties of the two systems. For isothermal problems, a number of approaches have been used to develop continuum models and to determine the appropriate relations. These approaches include 1) relating the force or deformation characteristics (or both) of a small segment of the lattice to those of a small segment of the continuum[1,2]; 2) using the discrete field method to obtain the governing difference equations of the lattice and either solving them directly[3] or converting them into approximate differential equations[4-6]; and 3) expanding the nodal displacements of a typical

(repeating) element of the lattice in Taylor series and equating the potential and kinetic energies of the lattice and continuum models.[7] This latter approach was found to work well for lattices with simple configurations. The approach was extended to thermoelastic problems in Ref. 8. However, for more complicated lattice configurations where the repeating element includes more than one bay, the predictions of the continuum models of Refs. 7 and 8 were found to be somewhat inaccurate. Careful examination of these situations revealed that certain local effects in the repeating element which were neglected in Refs. 7 and 8 must be incorporated to simulate accurately the response of complicated lattice structures. The present study focuses on this problem.

The objectives of the present paper are 1) to present a simple, rational method for developing continuum models which accounts for local effects in the repeating element, for large repetitive plate- and beamlike lattices subjected to static, thermal, and dynamic loadings (an extension and an improvement of the methods presented in Refs. 7 and 8); and 2) to demonstrate the accuracy of these models by means of numerical examples.

Development of the Energy Expressions for the Continuum Model

The first step in obtaining the expressions for the thermoelastic strain and kinetic energies of the continuum model is to isolate a typical (repeating) element of the original lattice grid. Then, the thermoelastic strain and kinetic energies of the repeating element are expressed in terms of the strains, temperatures, and nodal velocities as well, as the geometric and material properties of individual members. The transition from the discrete lattice structure to the continuum model is done by 1) introducing assumptions regarding the variation of the displacement components and temperature in the thickness direction for platelike lattices and in the plane of the cross section for beamlike lattices, 2) expressing the strains in the individual members in terms of the strain components in the coordinate directions which result from the assumed displacements, and 3) expanding each of the strain components in the coordinate directions in a Taylor series. The number of terms in the Taylor series is governed by the complexity of the problem and in no case should exceed the number of independent deformation modes in the lattice repeating element. This number is reduced further by requirements to insure compatibility at the interface of two repeating elements. The introduction of the displacement and temperature assumptions is the key element in replacing the three-dimensional lattice structure by a two- or one-dimensional continuum model. The replacement of the member strains by the Taylor series expansions of the strain components in the coordiante directions provides the transition from discrete structure to the continuum. The use of strain expressions rather than displacement expansions distinguishes the present approach from that presented in Refs. 7 and 8 and results in a greatly simplified expression for the thermoelastic strain energy of the continuum model.

Application to Beamlike Lattices

The proposed approach was applied to the beamlike lattices having triangular cross sections shown in Fig. 1. The continuum models for these lattices are one-dimensional beams. In each case, a typical element (chosen to be the smallest repeating element) is isolated from the grid. The triangular cross section provides the minimum number of longitudinal members but can result in undesirable skew deformations for certain reinforcing arrangements. These deformations are prevented by the use of the double lacings shown in Fig. 1a or by the use of the lacings shown in Figs. 1b and 1c. The repeating element of the lattice shown in Fig. 1a has double lacing and extends over one bay of the original structure, whereas the repeating elements of the lattices of Figs. 1b and

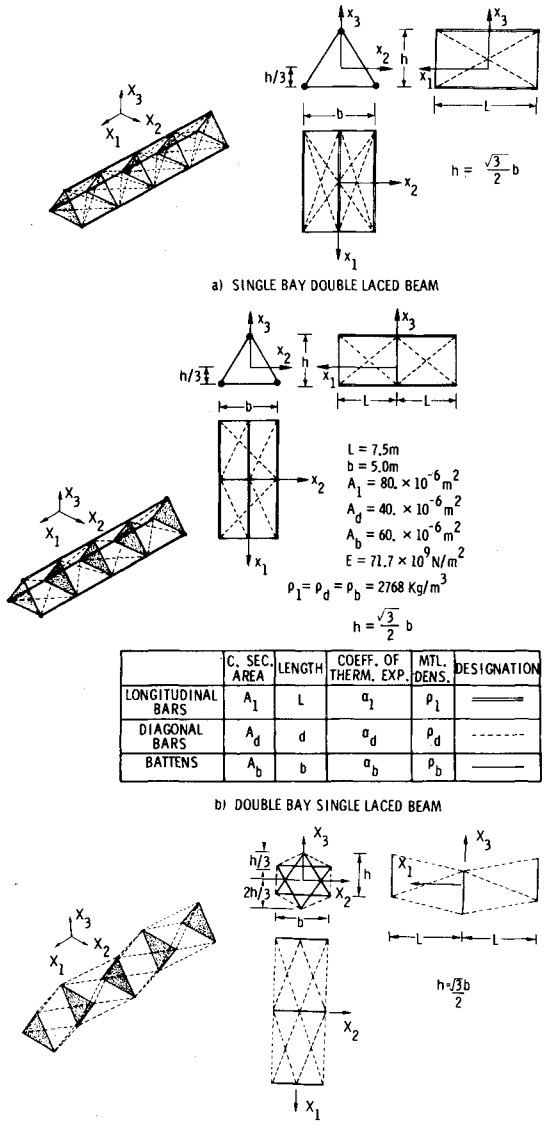

	C. SEC. AREA	LENGTH	COEFF. OF THERM. EXP.	MTL. DENS.	DESIGNATION
LONGITUDINAL BARS	A_l	L	α_l	ρ_l	———
DIAGONAL BARS	A_d	d	α_d	ρ_d	- - - - -
BATTENS	A_b	b	α_b	ρ_b	———

Fig. 1 Beamlike lattices used in present study.

1c have single lacing and extend over two bays of the original structures. All of the triangular frames formed by the battens in the first two lattices have the same orientation, but the triangular frames of the third lattice are rotated alternately 180 deg about the x_1 axis. Henceforth, the three lattices are referred to as single-bay, double-laced beams; double-bay, single-laced beams; and inverted batten beams, respectively.

Kinematic and Temperature Assumptions

Since each of the displacement components has a linear variation along the pin-connected members of the repeating element, the three displacement components of the lattice are assumed to have a linear variation in the plane of the cross section (plane x_2-x_3), i.e.,

$$u_1(x_1,x_2,x_3) = u_1^0 - x_2\phi_3 + x_3\phi_2 \tag{1a}$$

$$u_2(x_1,x_2,x_3) = u_2^0 + x_2\epsilon_2^0 + x_3[-\phi_1 + \tfrac{1}{2}(2\epsilon_{23}^0)] \tag{1b}$$

$$w(x_1,x_2,x_3) = w^0 + x_2[\phi_1 + \tfrac{1}{2}(2\epsilon_{23}^0)] + x_3\epsilon_3^0 \ \ldots \tag{1c}$$

where u_1^0, u_2^0, w^0 are the displacement components at $x_2 = x_3 = 0$; ϕ_1, ϕ_2, ϕ_3 are the rotation components; ϵ_2^0 and ϵ_3^0 are the extensional strains in the x_2 and x_3 directions; and $2\epsilon_{23}^0$ is the shearing strain in the plane of the cross section. The sign

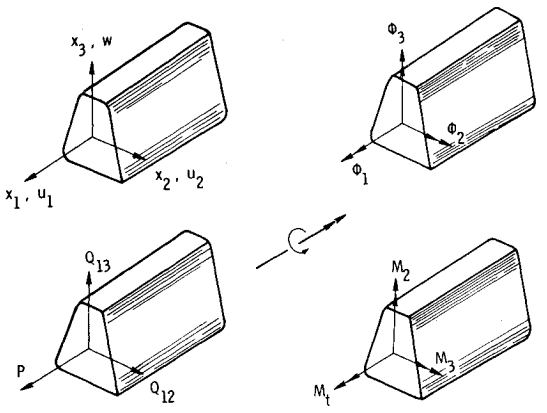

Fig. 2 Beam element and sign convention.

convention for the displacement and rotation components is shown in Fig. 2. The nine parameters u_1^0, u_2^0, w^0, ϕ_1, ϕ_2, ϕ_3, ϵ_2^0, ϵ_3^0, and $2\epsilon_{23}^0$ are functions of x_1 only.

For lattices with triangular cross section (such as the ones shown in Fig. 1), the deformed position of any cross section is specified completely by the three displacement components of its three nodes (a total of nine displacement parameters). Moreover, each of the displacement components has a linear variation in the x_2 and x_3 directions. Since there are a total of nine free parameters in the displacement expressions of Eqs. (1), these equations provide an exact representation of the displacement field for the lattices shown in Fig. 1.

As a consequence of the kinematic assumptions, Eqs. (1), the strain components have a linear variation in the x_2 and x_3 directions as follows:

$$\epsilon_{11} = \partial u_1^0 - x_2\partial\phi_3 + x_3\partial\phi_2 = \epsilon_1^0 - x_2\kappa_2^0 + x_3\kappa_3^0 \tag{2a}$$

$$\epsilon_{22} = \epsilon_2^0 \tag{2b}$$

$$\epsilon_{33} = \epsilon_3^0 \tag{2c}$$

$$2\epsilon_{12} = (\partial u_2^0 - \phi_3) + x_2\partial\epsilon_2^0 + x_3[-\partial\phi_1 + \tfrac{1}{2}\partial(2\epsilon_{23}^0)]$$

$$= 2\epsilon_{12}^0 + x_2\partial\epsilon_2^0 + x_3[-\kappa_1^0 + \tfrac{1}{2}\partial(2\epsilon_{23}^0)] \tag{2d}$$

$$2\epsilon_{13} = (\partial w^0 + \phi_2) + x_2[\partial\phi_1 + \tfrac{1}{2}\partial(2\epsilon_{23}^0)] + x_3\partial\epsilon_3^0$$

$$= 2\epsilon_{13}^0 + x_2[\kappa_1^0 + \tfrac{1}{2}\partial(2\epsilon_{23}^0)] + x_3\partial\epsilon_3^0 \tag{2e}$$

$$2\epsilon_{23} = 2\epsilon_{23}^0 \tag{2f}$$

where ϵ_1^0 is the extensional strain of the centerline; κ_2^0, κ_3^0 are the curvature changes in the x_2 and x_3 directions; κ_1^0 is the twist; $2\epsilon_{12}^0$ and $2\epsilon_{13}^0$ are the transverse shear strains; and $\partial \equiv \mathrm{d}/\mathrm{d}x_1$. The strain measures $\epsilon_1^0, \epsilon_2^0, \epsilon_3^0, 2\epsilon_{12}^0, 2\epsilon_{13}^0, 2\epsilon_{23}^0, \kappa_2^0, \kappa_3^0$, and κ_1^0 are functions of x_1 only.

The temperature distribution also is assumed to be linear in the x_2 and x_3 directions, i.e.,

$$T(x_1, x_2, x_3) = T^0 + x_2\partial_2 T^0 + x_3\partial_3 T^0 \tag{3}$$

where T^0 is the temperature at $x_2 = x_3 = 0$; and $\partial_2 T^0 \equiv \partial T^0/\partial x_2$, $\partial_3 T^0 \equiv \partial T^0/\partial x_3$ are the temperature gradients in the x_2 and x_3 directions.

Strain Expansions

The axial strain in each member of the repeating element is replaced by its expression in terms of the strain components in the coordinate directions, i.e.,

$$\epsilon^{(k)} = \sum_{i=1}^{3}\sum_{j=1}^{3} \epsilon_{ij}^{(k)} \ell_i^{(k)} \ell_j^{(k)} \tag{4}$$

where $\epsilon^{(k)}$ is the axial strain in a typical member; $\epsilon_{ij}^{(k)}$ are the strain components in the coordinate directions evaluated at the center of the member; and $\ell_i^{(k)}$ are the direction cosines of the member k.

The strain components in the coordinate directions $\epsilon_{ij}^{(k)}$ are expanded in a Taylor series about a suitably chosen origin as follows:

$$\epsilon_{11}^{(k)} \simeq \epsilon_1^0 - x_2^{(k)}\kappa_2^0 + x_3^{(k)}\kappa_3^0 + x_1^{(k)}(\partial\epsilon_1^0 - x_2^{(k)}\partial\kappa_2^0 + x_3^{(k)}\partial\kappa_3^0) \tag{5a}$$

$$\epsilon_{22}^{(k)} \simeq \epsilon_2^0 + x_1^{(k)}\partial\epsilon_2^0 + \tfrac{1}{2}(x_1^{(k)})^2\,\partial^2\epsilon_2^0 \tag{5b}$$

$$\epsilon_{33}^{(k)} \simeq \epsilon_3^0 + x_1^{(k)}\partial\epsilon_3^0 + \tfrac{1}{2}(x_1^{(k)})^2\,\partial^2\epsilon_3^0 \tag{5c}$$

$$2\epsilon_{12}^{(k)} \simeq 2\epsilon_{12}^0 + x_2^{(k)}\partial\epsilon_2^0 + x_3^{(k)}[-\kappa_1^0 + \tfrac{1}{2}\partial(2\epsilon_{23}^0)]$$

$$+ x_1^{(k)}\{\partial(2\epsilon_{12}^0) + x_2^{(k)}\partial^2\epsilon_2^0 + x_3^{(k)}[-\partial\kappa_1^0 + \tfrac{1}{2}\partial^2(2\epsilon_{23}^0)]\} \tag{5d}$$

$$2\epsilon_{13}^{(k)} \simeq 2\epsilon_{13}^0 + x_2^{(k)}[\kappa_1 + \tfrac{1}{2}\partial(2\epsilon_{23}^0)] + x_3^{(k)}\partial\epsilon_3^0$$

$$+ x_1^{(k)}\{\partial(2\epsilon_{13}^0) + x_2^{(k)}[\partial\kappa_1^0 + \tfrac{1}{2}\partial^2(2\epsilon_{23}^0)] + x_3^{(k)}\partial^2\epsilon_3^0\} \tag{5e}$$

$$2\epsilon_{23}^{(k)} \simeq 2\epsilon_{23}^0 + x_1^{(k)}\partial(2\epsilon_{23}^0) + \tfrac{1}{2}(x_1^{(k)})^2\,\partial^2(2\epsilon_{23}^0) \tag{5f}$$

where $x_1^{(k)}, x_2^{(k)}$, and $x_3^{(k)}$ are the coordinates of the center of the kth member, and $\partial^2 \equiv \mathrm{d}^2/\mathrm{d}x_1^2$.

Compatibility between repeating elements of the beam model requires that the strain components in the plane of the cross sections of two adjacent elements ($\epsilon_{22}, \epsilon_{33}$, and $2\epsilon_{23}$) be identical at their interface. This condition is satisfied if the odd-order derivatives of these strain components [singly underlined terms in Eqs. (5)] are set equal to zero, i.e.,

$$\partial\epsilon_2^0 = \partial\epsilon_3^0 = \partial(2\epsilon_{23}^0) = 0 \tag{6}$$

Compatibility conditions, Eq. (6), can be verified easily for the simple loading cases of pure axial force, pure bending, and transverse loading.

For lattices with a single-bay repeating element (such as the one shown in Fig. 1a), there are 12 independent deformation modes that correspond to the zeroth-order terms in the Taylor series expansions. And since there are three compatibility conditions, Eqs. (6), the total number of strain components which can be used in this Taylor series expansion, Eqs. (5), reduces to nine. This is equivalent to assuming a uniform state of strain $\epsilon_1^0, \kappa_2^0, \kappa_3^0, 2\epsilon_{12}^0, 2\epsilon_{13}^0, \kappa_1^0, \epsilon_2^0, \epsilon_3^0, 2\epsilon_{23}^0$ within each repeating element.

For lattices with two bays in their repeating element (such as the ones shown in Figs. 1b and 1c), an additional nine strain parameters are possible. If all of the first-order terms in the Taylor series expansion are added (terms linear in x_1), a total of nine first derivatives of strain components and the three second derivatives $\partial^2\epsilon_2^0, \partial^2\epsilon_3^0$, and $\partial^2(2\epsilon_{23}^0)$ appear. The first-order terms involving $\epsilon_2^0, \epsilon_3^0$, and $(2\epsilon_{23}^0)$ again are set equal to zero because of compatibility. This reduces the number of additional strain parameters to the nine possible ones. Therefore, the total possible strain parameters in a two-bay repeating element is equal to 18. However, in order to account fully for the contributions of the second derivatives $\partial^2\epsilon_2^0, \partial^2\epsilon_3^0$, and $\partial^2(2\epsilon_{23}^0)$, the second-order terms of the Taylor series expansions of $\epsilon_{22}, \epsilon_{23}$ and $2\epsilon_{23}$ [doubly underlined terms in Eqs. (5)] must be included.

Thermoelastic Strain Energy

The thermoelastic strain energy of the repeating element is given by

$$\bar{U} = \frac{1}{2}\sum_{\text{members}} E^{(k)}A^{(k)}L^{(k)}(\epsilon^{(k)} - \alpha^{(k)}T^{(k)})^2 \tag{7}$$

where $\epsilon^{(k)}$ is the axial strain of a typical bar k; E, A, L, α, and T are the elastic modulus, cross-sectional area, length, coefficient of thermal expansion, and average temperature of member k.

If $\epsilon^{(k)}$ in Eq. (7) is replaced by its expression in terms of the different strain components, Eqs. (4) and (5), the thermoelastic strain energy of the repeating element $\bar{U}$ can be written as a function of the strain gradients, as well as the strain components and temperature.

Inclusion of the strain gradients is the key to obtaining correct stiffnesses for more complicated configurations, especially those having more than one bay in a repeating element. For example, the planar truss configuration under end loading shown in Fig. 3 undergoes deformation, as shown by the dashed lines. On the average it remains straight, but locally a zig-zag pattern occurs. The use of strain gradients allows such a pattern.

Since, in general, such local deformation should be allowed to occur freely, the forces associated with it should be zero. This can be accomplished by setting the derivatives of the energy with respect to the strain gradients equal to zero, i.e.,

$$\frac{\partial\bar{U}}{\partial[\partial\epsilon_1^0]}=\frac{\partial\bar{U}}{\partial[\partial\kappa_2^0]}=\frac{\partial\bar{U}}{\partial[\partial\kappa_3^0]}=\frac{\partial\bar{U}}{\partial[\partial(2\epsilon_{12}^0)]}=\frac{\partial\bar{U}}{\partial[\partial(2\epsilon_{13}^0)]}$$

$$=\frac{\partial\bar{U}}{\partial[\partial\kappa_1^0]}=\frac{\partial\bar{U}}{\partial[\partial^2\epsilon_2^0]}=\frac{\partial\bar{U}}{\partial[\partial^2\epsilon_3^0]}=\frac{\partial\bar{U}}{\partial[\partial^2(2\epsilon_{23}^0)]}=0 \tag{8}$$

Moreover, in order to obtain a shear-deformation-type beam theory, the forces associated with the strain components in the plane of the cross section are set equal to zero, i.e.,

$$\frac{\partial\bar{U}}{\partial\epsilon_2^0}=\frac{\partial\bar{U}}{\partial\epsilon_3^0}=\frac{\partial\bar{U}}{\partial(2\epsilon_{23}^0)}=0 \tag{9}$$

Equations (8) and (9) can be used to express the strain gradients and the strain components $\epsilon_2^0,\epsilon_3^0,2\epsilon_{23}^0$ in terms of the other strain components and temperatures, thereby reducing the thermoelastic strain energy to a quadratic form in the six strain components $\epsilon_1^0,\kappa_2^0,\kappa_3^0,2\epsilon_{12}^0,2\epsilon_{13}^0,\kappa_t^0$ and temperature only. The resulting expression of the thermoelastic strain energy can be written in the following form:

$$\bar{U}=U-U_\ell-U_q \tag{10}$$

where U is the isothermal strain energy; U_ℓ and U_q are contributions of the linear and quadratic terms in T^0, $\partial_2 T^0$ and $\partial_3 T^0$, to the strain energy. The quantity U_q is free of displacements and rotations and, therefore, has no contribution to the equations of motion. The quantity U_ℓ is linear in the displacements and rotations. The expressions of U and U_ℓ are given by

$$U=\tfrac{1}{2}\bar{L}\{\epsilon\}^t[C]\{\epsilon\} \tag{11a}$$

$$U_\ell=\bar{L}\{\epsilon\}^t\{C_T\} \tag{11b}$$

where

$$\{\epsilon\}^t=[\epsilon_1^0\ \ \kappa_2^0\ \ \kappa_3^0\ \ 2\epsilon_{12}^0\ \ 2\epsilon_{13}^0\ \ \kappa_t^0]$$

$\bar{L}$ is the length of the repeating element, $[C]$ is the 6×6 matrix of stiffness coefficients; $\{C_T\}$ is a vector of effective thermoelastic stiffnesses of the beam model; and superscript t denotes transposition. The thermoelastic coefficients $[C]$ and $\{C_T\}$ for the three grids shown in Fig. 1 are given in Table 1. In this table, C_{11} refers to the extensional stiffness of the beam; C_{22} and C_{33} are the bending stiffnesses; C_{44} and C_{55} are the transverse shear stiffnesses; and C_{66} is the torsional stiffness.

Table 1 Thermoelastic and dynamic coefficients for the beam models of the lattice grids shown in Fig. 1

	Single-bay double-laced beam	Double-bay single-laced beam	Inverted batten beam
$\bar{L}$	L	$2L$	$2L$
C_{11}	$\frac{3}{\mu}\left(E_lA_l\mu+2\frac{L^3}{d^3}E_dA_d\right)$	$3E_lA_l$	$\frac{6}{1+(5/18)\gamma}\frac{L^3}{d^3}E_dA_d$
$C_{22}=C_{33}$	$\frac{b^2}{2\mu}\left(E_lA_l\mu+\frac{1}{2}\frac{L^3}{d^3}E_dA_d\right)$	$\frac{b^2}{2}E_lA_l$	$\frac{3b^2}{4(1+\frac{1}{2}\gamma)}\frac{L^3}{d^3}E_dA_d$
$C_{44}=C_{55}$	$3\frac{b^2L}{d^3}E_dA_d$	$\frac{3}{2(1+\frac{1}{4}\lambda)}\frac{b^2L}{d^3}E_dA_d$	$\frac{b^2L}{d^3}E_dA_d$
C_{66}	$\frac{1}{2}\frac{b^4L}{d^3}E_dA_d$	$\frac{1}{4(1+\lambda)}\frac{b^4L}{d^3}E_dA_d$	$\frac{1}{2}\frac{b^4L}{d^3}E_dA_d$
m_0	$3\left(\rho_lA_l+\frac{b}{L}\rho_bA_b+2\frac{d}{L}\rho_dA_d\right)$	$3\left(\rho_lA_l+\frac{b}{L}\rho_bA_b+\frac{d}{L}\rho_dA_d\right)$	$3\left(\frac{b}{L}\rho_bA_b+2\frac{d}{L}\rho_dA_d\right)$
$m_{22}=m_{33}$	$\frac{b^2}{2}\left(\rho_lA_l+\frac{1}{2}\frac{b}{L}\rho_bA_b+\frac{d}{L}\rho_dA_d\right)$	$\frac{b^2}{2}\left(\rho_lA_l+\frac{1}{2}\frac{b}{L}\rho_dA_b+\frac{1}{2}\frac{d}{L}\rho_dA_d\right)$	$\frac{b^2}{2}\left(\frac{1}{2}\frac{b}{L}\rho_bA_b+\frac{5}{3}\frac{d}{L}\rho_dA_d\right)$
C_{T1}/T^0	$\frac{3}{\mu}\left[\alpha_lE_lA_l\mu+2\frac{L}{d}E_dA_d\left(\alpha_d-\frac{b^2}{d^2}\alpha_b\right)\right]$	$3\alpha_lE_lA_l$	$\frac{2}{1+(5/18)\gamma}\frac{L}{d}E_dA_d\left(3\alpha_d-\frac{b^2}{d^2}\alpha_b\right)$
$C_{T2}/\partial_2T^0=$ $-C_{T3}/\partial_3T^0$	$-\frac{b^2}{2\mu}\left[\alpha_lE_lA_l\mu+\frac{1}{2}\frac{L}{d}E_dA_d\left(\alpha_d-\frac{b^2}{d^2}\alpha_b\right)\right]$	$-\frac{b^2}{2}\alpha_lE_lA_l$	$\frac{-b^2}{4(1+2/3\gamma)}\frac{L}{d}E_dA_d\left(3\alpha_d-\frac{b^2}{d^2}\alpha_b\right)$

$$\mu=1+2\frac{b^3}{d^3}\frac{E_dA_d}{E_bA_b},\qquad \lambda=\frac{L^3}{d^3}\frac{E_dA_d}{E_lA_l},\qquad \gamma=\frac{b^3}{d^3}\frac{E_dA_d}{E_bA_b}$$

Comments on the Thermoelastic Characteristics of the Beam Models

In obtaining the thermoelastic characteristics of the three grids shown in Fig. 1, the following observations were noted:

1) For the inverted batten beams shown in Fig. 1c, the second derivatives of the strain components $\epsilon_2^0, \epsilon_3^0$, and $2\epsilon_{23}^0$ must be included in the Taylor series expansions, Eqs. (7), in order for the batten members to participate in the transverse load-carrying ability of the beam as observed for the actual structure. When the second derivatives are included, the batten members contribute to the bending stiffnesses of the beam model. On the other hand, the stiffness coefficients of the double-bay, single-laced beam shown in Fig. 1b are not affected by the inclusion of the second derivatives.

2) A classcial beam theory can be obtained from the shear deformation beam theory used in the present study by setting the transverse shear strains = 0, i.e.,

$$2\epsilon_{12}^0 = \partial u_2^0 - \phi_3 = 0 \tag{12a}$$

$$2\epsilon_{13}^0 = \partial w^0 + \phi_2 = 0 \tag{12b}$$

Kinetic Energy

If a consistent mass approach is used, the kinetic energy of the repeating element can be expressed as follows:

$$K = \frac{1}{6}\omega^2 \sum_{\text{members}} \rho^{(k)} A^{(k)} L^{(k)} [(u_1^i)^2 + u_1^i u_1^j + (u_1^j)^2 + (u_2^i)^2 + u_2^i u_2^j + (u_2^j)^2 + (w^i)^2 + w^i w^j + (w^j)^2] \tag{13}$$

where ρ is the mass density of a typical bar k joining nodes i and j, and ω is the circular frequency of vibration.

If Eqs. (1) are used and the inertia terms associated with the strain components $\epsilon_2^0, \epsilon_3^0$, and $2\epsilon_{23}^0$ are neglected, the kinetic energy of the beam model can be written in the following form:

$$K = \tfrac{1}{2}\bar{L}\omega^2 [m_0 (u_1^0 u_1^0 + u_2^0 u_2^0 + w^0 w^0) + 2m_{02}(-u_1^0 \phi_3 + w^0 \phi_1) + 2m_{03}(u_1^0 \phi_2 - u_2^0 \phi_1) - 2m_{23}\phi_2\phi_3 + m_{22}(\phi_1\phi_1 + \phi_3\phi_3) + m_{33}(\phi_1\phi_1 + \phi_2\phi_2)] \tag{14}$$

where $m_0, m_{02}, m_{03}, m_{23}, m_{22}$, and m_{33} are density parameters of the beam; and ω is the circular frequency of vibration of the beam.

Work Done by External Forces

The expression for the work done by external forces, consistent with the kinematic assumptions, Eqs. (1), is

$$W = \sum_i [P_1^i (u_1^0 - x_2^i \phi_3 + x_3^i \phi_2) + P_2^i \{u_2^0 + x_2^i \epsilon_2^0 + x_3^i [-\phi_1 + \tfrac{1}{2}(2\epsilon_{23}^0)]\} + P_3^i \{w^0 + x_2^i [\phi_1 + \tfrac{1}{2}(2\epsilon_{23}^0)] + x_3^i \epsilon_3^0\}] \tag{15}$$

where P_1^i, P_2^i, and P_3^i are the external load components in the coordinate directions at a typical node i, and the summation extends over all points of application of the external forces.

Application to Platelike Lattices

In this section, applications of the proposed approach to the hexahedral and tetrahedral grids shown in Figs. 4a and 4b are outlined. The tetrahedral grid has many attractive features for application to large-area space structures, and many of its stiffness characteristics have been derived by other methods. The hexahedral grid contains many more redundancies and has vertical members that present difficulties in some approaches. Therefore, the hexahedral grid provides a good check on the versatility and reliability of the approach presented herein. In each case, a typical repeating element is isolated from the grid. The continuum model in this case is a two-dimensional plate continuum. For convenience and conciseness, index notation is used throughout this section.

Kinematic and Temperature Assumptions

The three displacement components u_1, u_2, and w are assumed to have a linear variation in the thickness coordinate x_3, i.e.,

$$\left.\begin{aligned} u_\alpha(x_\beta, x_3) &= u_\alpha^0 + x_3\phi_\alpha \\ w(x_\beta, x_3) &= w^0 + x_3\epsilon_3^0 \end{aligned}\right\} \alpha,\beta = 1,2 \tag{16}$$

where u_α^0 and w^0 are the displacement components at $x_3 = 0$, ϕ_α are the rotation components, and ϵ_3^0 is the transverse normal strain in the x_3 direction. The sign convention for the displacement and rotation components is shown in Fig. 5. Equations 16 represent the exact displacement variation in the thickness direction provided that no internal nodes are present.

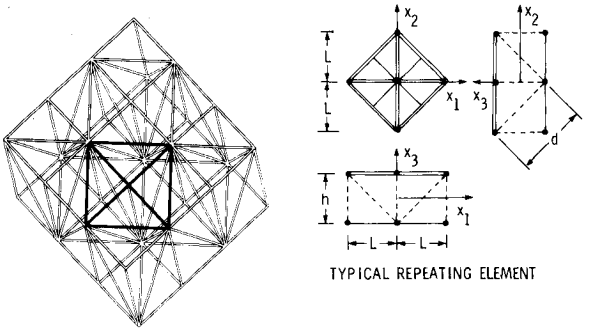

$A_1 = 80 \times 10^{-6}\ m^2$, $E = 71.7 \times 10^9\ N/m^2$
$A_2 = 50 \times 10^{-6}\ m^2$, $\alpha_1 = \alpha_2 = \alpha_d = \alpha_v$
$A_d = 10 \times 10^{-6}\ m^2$ $= 18 \times 10^{-6}/°C$
$A_v = 10 \times 10^{-6}\ m^2$, $\rho_1 = \rho_2 = \rho_d = \rho_v$
$L = 7.5\ m$ $= 2768\ kg/m^3$
$h = 7.5\ m$

	CROSS SEC. AREA	LG.	COEFF. OF THERM. EXP.	MATL. DENS.	DES.
TOP SURF. BARS	A_1	$L, \sqrt{2}L$	α_1	ρ_1	═══
BOTTOM SURF. BARS	A_2	$L, \sqrt{2}L$	α_2	ρ_2	———
VERTICALS	A_v	h	α_v	ρ_v	- - - -
DIAGONALS	A_d	d	α_d	ρ_d	- - - -

a) HEXAHEDRAL GRID

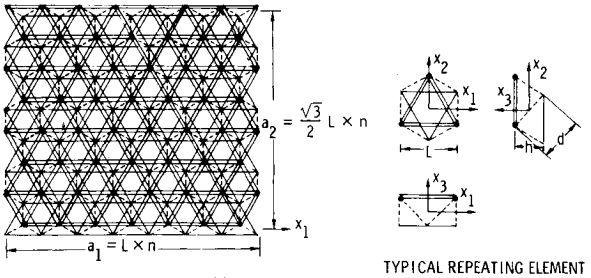

b) TETRAHEDRAL GRID

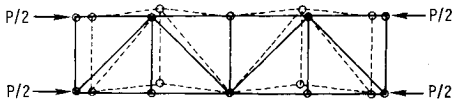

Fig. 3 Deformation of axially loaded lattice truss.

Fig. 4 Double-layered grids used in present study.

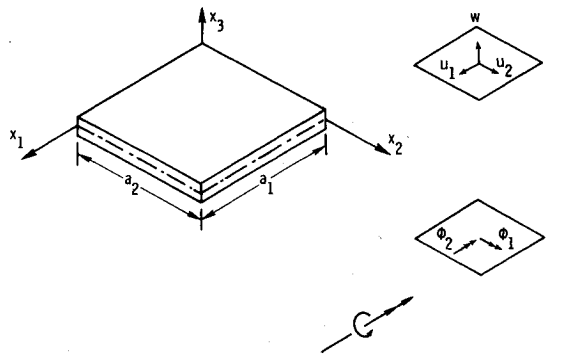

Fig. 5 Plate element and sign convention.

As a consequence of the displacement assumptions, Eqs. (16), the strain components have a linear variation across the thickness of the plate as follows:

$$\epsilon_{\alpha\beta} = \tfrac{1}{2}(\partial_\alpha u^0_\beta + \partial_\beta u^0_\alpha) + x_3 \tfrac{1}{2}(\partial_\alpha \phi_\beta + \partial_\beta \phi_\alpha)$$

$$= \epsilon^0_{\alpha\beta} + x_3 \kappa^0_{\alpha\beta} \tag{17a}$$

$$\epsilon_{33} = \epsilon^0_3 \tag{17b}$$

$$2\epsilon_{\alpha 3} = (\partial_\alpha w^0 + \phi_\alpha) + x_3 \partial_\alpha \epsilon^0_3 = 2\epsilon^0_{\alpha 3} + x_3 \partial_\alpha \epsilon^0_3 \tag{17c}$$

where $\epsilon^0_{\alpha\beta}$ are the extensional strains of the middle plane; ϵ^0_3 is the transverse normal strain of the middle plane; $\kappa^0_{\alpha\beta}$ are the curvature changes and twist; and $2\epsilon^0_{\alpha 3}$ are the transverse shear strains. The strain measures $\epsilon^0_{\alpha\beta}, \kappa^0_{\alpha\beta}, \epsilon^0_3$, and $2\epsilon^0_{\alpha 3}$ are independent of x_3

The temperature distribution also is assumed to be linear in the x_3 direction, i.e.,

$$T(x_\beta, x_3) = T^0(x_\beta) + x_3 \ \partial_3 T^0(x_\beta) \tag{18}$$

where T^0 is the temperature at $x_3 = 0$, and $\partial_3 T^0 \equiv \partial T^0 / \partial x_3$ is the temperature gradient in the x_3 direction.

Strain Expansions

The thermoelastic strain energy of the plate continuum is obtained by first replacing the axial strain in each member of the repeating element by its expression in terms of the strain components in the coordinate directions $\epsilon^{(k)}_{ij}$, Eqs. (4), and then expanding $\epsilon^{(k)}_{ij}$ in Taylor series about a suitably chosen origin. For the two grids shown in Figs. 4a and 4b, the following truncated Taylor series were used:

$$\epsilon^{(k)}_{\alpha\beta} \cong \epsilon^0_{\alpha\beta} + x^{(k)}_3 \kappa^0_{\alpha\beta} + \sum_{\gamma=1}^{2} x_\gamma{}^{(k)} (\partial_\gamma \epsilon^0_{\alpha\beta} + x^{(k)}_3 \partial_\gamma \kappa^0_{\alpha\beta}) \tag{19a}$$

$$\epsilon^{(k)}_{33} \cong \epsilon^0_3 + \sum_{\alpha=1}^{2} x^{(k)}_\alpha \partial_\alpha \epsilon^0_3 \tag{19b}$$

$$2\epsilon^{(k)}_{\alpha 3} \cong 2\epsilon^0_{\alpha 3} + x^{(k)}_3 \partial_\alpha \epsilon^0_3 + \sum_{\gamma=1}^{2} x^{(k)}_\gamma [\partial_\gamma (2\epsilon^0_{\alpha 3}) + x^{(k)}_3 \partial_\gamma \partial_\alpha \epsilon^0_3] \tag{19c}$$

where $x^{(k)}_\alpha$ and $x^{(k)}_3$ are the coordinates of the center of the kth member.

The number of strain terms to be included in the Taylor series expansion can be determined by consideration of the independent deformation modes of the repeating element and the compatibility conditions with adjacent elements, as was done in the preceding section for beamlike lattices. For the tetrahedral grid, only the zeroth-order terms in the Taylor series expansion were included, and $\partial_\alpha \epsilon^0_3$ was set equal to zero to satisfy the compatibility conditions with adjacent elements.

For the hexahedral grid, the following first-order terms in the Taylor series expansion also were included: $\partial_\gamma (2\epsilon^0_{\alpha 3})$, $\partial_\gamma \partial_\alpha \epsilon^0_3$, and $\partial_\gamma \kappa^0_{\alpha\beta}$. However, the latter two did not contribute to the stiffness coefficients.

Thermoelastic Strain Energy

The expression for the thermoelastic strain energy for the two grids shown in Fig. 4 can be written in the following form:

$$\bar{U} = \bar{U}[\epsilon^0_{\alpha\beta}, \epsilon^0_3, \kappa^0_{\alpha\beta}, 2\epsilon^0_{\alpha 3}, \partial_\gamma (2\epsilon^0_{\alpha 3}), \partial_\gamma \kappa^0_{\alpha\beta}, \partial_\gamma \partial_\alpha \epsilon^0_3, T^0, \partial_3 T^0] \tag{20}$$

Inclusion of the gradients of the transverse shear strain measures $2\epsilon^0_{\alpha 3}$ and $\partial_\alpha \epsilon^0_3$ is the key to obtaining correct stiffnesses for complicated double-layered grids such as the hexahedral grid. Since deformations associated with $\partial_\gamma (2\epsilon^0_{\alpha 3})$ and $\partial_\gamma \partial_\alpha \epsilon^0_3$ should be allowed to occur freely, the forces associated with such deformations should be zero, i.e.,

$$\frac{\partial \bar{U}}{\partial [\partial_\gamma (2\epsilon^0_{\alpha 3})]} = \frac{\partial \bar{U}}{\partial [\partial_\gamma \partial_\alpha \epsilon^0_3]} = 0 \tag{21}$$

Moreover, to obtain a shear-deformation-type plate theory, the stress resultant associated with ϵ^0_3 is set equal to zero, i.e.,

$$\frac{\partial \bar{U}}{2\epsilon^0_3} = 0 \tag{22}$$

Equations (21) and (22) can be used to express the strain gradients and the strain component ϵ^0_3 in terms of the other strain components and temperatures, thereby reducing the thermoelastic strain energy to a quadratic form in the strain components $\epsilon^0_{\alpha\beta}, \kappa^0_{\alpha\beta}, 2\epsilon^0_{\alpha 3}$ and temperatures $T^0, \partial_3 T^0$.

The resulting expression of the thermoelastic strain energy can be written in the following form:

$$\bar{U} = U - U_\ell - U_q \tag{23}$$

where U is the isothermal strain energy; U_ℓ and U_q are the contributions of the linear and quadratic terms in T^0 and $\partial_3 T^0$ to the strain energy. The expressions for U and U_ℓ are given by

$$U = \tfrac{1}{2} a[C_{\alpha\beta\gamma\rho} \epsilon^0_{\alpha\beta} \epsilon^0_{\gamma\rho} \text{ (extensional strain energy)}$$

$$+ D_{\alpha\beta\gamma\rho} \kappa^0_{\alpha\beta} \kappa^0_{\gamma\rho} \text{ (bending strain energy)}$$

$$+ C_{\alpha 3\beta 3} (2\epsilon^0_{\alpha 3})(2\epsilon^0_{\beta 3}) \text{ (transverse shear strain energy)}$$

$$+ 2F_{\alpha\beta\gamma\rho} \epsilon^0_{\alpha\beta} \kappa^0_{\gamma\rho} \text{ (bending-extensional coupling)}$$

$$+ 2F_{\alpha 3\beta\gamma} (2\epsilon^0_{\alpha 3}) \epsilon^0_{\beta\gamma}] \text{ (transverse shear-extensional coupling)} \tag{24a}$$

$$U_\ell = a\{[C_{T\alpha\beta} \epsilon^0_{\alpha\beta} + F_{T\alpha\beta} \kappa^0_{\alpha\beta} + C_{T\alpha 3} (2\epsilon^0_{\alpha 3})] T^0$$

$$+ [F_{T\alpha\beta} \epsilon^0_{\alpha\beta} + D_{T\alpha\beta} \kappa^0_{\alpha\beta}] \partial_3 T^0\} \tag{24b}$$

where a is the planform area of the repeating element; $C_{\alpha\beta\gamma\rho}$ ($\alpha, \beta, \gamma, \rho = 1, 2$) are extensional stiffnesses; $D_{\alpha\beta\gamma\rho}$ are bending stiffnesses; $F_{\alpha\beta\gamma\rho}$ are bending-extensional coupling coefficients of the plate; $C_{\alpha 3\beta 3}$ are transverse shear stiffnesses of the plate; the coefficients C_T, F_T, and D_T are effective thermoelastic stiffnesses of the plate model; and a repeated Greek index denotes summation over the range 1, 2.

Kinetic Energy

If the inertia terms associated with the transverse normal strain ϵ^0_3 are neglected, the kinetic energy can be written in the

Table 2 Elastic and dynamic coefficients for tetrahedral and hexahedral grids

	Tetrahedral grid	Hexahedral grid
a	$\frac{\sqrt{3}}{2}L^2$	$2L^2$
$C_{1111}=C_{2222}$	$\frac{3\sqrt{3}}{4}\frac{1}{L}\left(E_1A_1+E_2A_2+\frac{1}{27}\frac{L^3}{d^3}E_dA_d\right)$	$\frac{1}{L}\left(1+\frac{1}{2\sqrt{2}}\right)(E_1A_1+E_2A_2)$
C_{1122}	$\frac{\sqrt{3}}{4}\frac{1}{L}\left(E_1A_1+E_2A_2-\frac{1}{9}\frac{L^3}{d^3}E_dA_d\right)$	$\frac{1}{2\sqrt{2}}\frac{1}{L}(E_1A_1+E_2A_2)$
C_{1212}	$\frac{\sqrt{3}}{4}\frac{1}{L}\left(E_1A_1+E_2A_2+\frac{1}{9}\frac{L^3}{d^3}E_dA_d\right)$	$\frac{1}{2\sqrt{2}}\frac{1}{L}(E_1A_1+E_2A_2)$
$\tilde{C}_{1133}=\tilde{C}_{2233}$	$\frac{1}{\sqrt{3}}\frac{h^2}{d^3}E_dA_d$	0
$\tilde{C}_{3333}$	$2\sqrt{3}\frac{h^4}{d^3L^2}E_dA_d$	$\frac{h}{L^2}E_vA_v$
$F_{1111}=F_{2222}$	$\frac{3\sqrt{3}}{8}\frac{h}{L}(E_1A_1-E_2A_2)$	$\frac{h}{2L}\left(1+\frac{1}{2\sqrt{2}}\right)(E_1A_1-E_2A_2)$
$F_{1122}=F_{1212}$	$\frac{\sqrt{3}}{8}\frac{h}{L}(E_1A_1-E_2A_2)$	$\frac{1}{4\sqrt{2}}\frac{h}{L}(E_1A_1-E_2A_2)$
$D_{1111}=D_{2222}$	$3\frac{\sqrt{3}}{16}\frac{h^2}{L}(E_1A_1+E_2A_2)$	$\frac{h^2}{4L}\left(1+\frac{1}{2\sqrt{2}}\right)(E_1A_1+E_2A_2)$
$D_{1122}=D_{1212}$	$\frac{\sqrt{3}}{16}\frac{h^2}{L}(E_1A_1+E_2A_2)$	$\frac{h^2}{8\sqrt{2}L}(E_1A_1+E_2A_2)$
$C_{1313}=C_{2323}$	$\frac{1}{\sqrt{3}}\frac{h^2}{d^3}E_dA_d$	$\frac{h^2}{d^3}E_dA_d$
$F_{1312}=F_{2311}$ $=-F_{2322}$	$-\frac{1}{6}\frac{hL}{d^3}E_dA_d$	0
m_0	$2\sqrt{3}\frac{1}{L}(\rho_1A_1+\rho_2A_2+\frac{d}{L}\rho_dA_d)$	$\frac{2}{L}\left[\left(1+\frac{1}{\sqrt{2}}\right)(\rho_1A_1+\rho_2A_2)+\frac{1}{2}\frac{h}{L}\rho_vA_v+\frac{d}{L}\rho_dA_d\right]$
m_1	$\sqrt{3}\frac{h}{L}(\rho_1A_1-\rho_2A_2)$	$\frac{h}{L}\left[\left(1+\frac{1}{\sqrt{2}}\right)(\rho_1A_1-\rho_2A_2)\right]$
m_2	$\frac{\sqrt{3}}{2}\frac{h^2}{L}\left(\rho_1A_1+\rho_2A_2+\frac{1}{3}\frac{d}{L}\rho_dA_d\right)$	$\frac{h^2}{2L}\left[\left(1+\frac{1}{\sqrt{2}}\right)(\rho_1A_1+\rho_2A_2)+\frac{1}{6}\frac{h}{L}\rho_vA_v+\frac{1}{3}\frac{d}{L}\rho_dA_d\right]$
$C_{T11}=C_{T22}$	$\frac{\sqrt{3}}{L}\left(\alpha_1E_1A_1+\alpha_2E_2A_2+\frac{1}{3}\frac{L}{d}\alpha_dE_dA_d\right)$	$\frac{1}{L}\left(1+\frac{1}{\sqrt{2}}\right)(\alpha_1E_1A_1+\alpha_2E_2A_2)$
$\tilde{C}_{T33}$	$2\sqrt{3}\frac{h^2}{dL^2}\alpha_dE_dA_d$	$\frac{h}{L^2}\alpha_vE_vA_v$
$F_{T11}=F_{T22}$	$\frac{\sqrt{3}}{2}\frac{h}{L}(\alpha_1E_1A_1-\alpha_2E_2A_2)$	$\frac{h}{2L}\left(1+\frac{1}{\sqrt{2}}\right)(\alpha_1E_1A_1-\alpha_2E_2A_2)$
$D_{T11}=D_{T22}$	$\frac{\sqrt{3}}{4}\frac{h^2}{L}(\alpha_1E_1A_1+\alpha_2E_2A_2)$	$\frac{h^2}{4L}\left(1+\frac{1}{\sqrt{2}}\right)(\alpha_1E_1A_1+\alpha_2E_2A_2)$

following form:

$$K=\tfrac{1}{2}a\omega^2[m_0(u_\alpha^0u_\alpha^0+w^0w^0)+2m_1u_\alpha^0\phi_\alpha+m_2\phi_\alpha\phi_\alpha] \quad (25)$$

where a is the planform area of the repeating element; m_0, m_1, and m_2 are density parameters of the plate; and ω is the circular frequency of vibration of the plate. The elastic, thermal, and dynamic coefficients of the two grids shown in Figs. 4a and 4b are given in Table 2. For the tetrahedral grid, the corresponding coefficients based on the theory of Refs. 7 and 8 are given in the cited references.

Table 3 Comparison of maximum displacements and minimum vibration frequencies (in hertz) obtained by the continuum beam models with exact solutions for the lattices shown in Fig. 1. Numbers of bays = 10

	Single-bay double-laced		Double-bay single-laced		Inverted batten	
	Beam model	Exact	Beam model	Exact	Beam model	Exact
$10^5 \times u_1^0/P$ (m/N)	0.297	0.296	0.436	0.436	0.292	0.286
$10^2 \times w^0/Q_{13}$ (m/N)	0.179	0.178	0.203	0.203	0.199	0.194
$10^5 \times \phi_1/M_1$ $(m/N)^{-1}$	0.817	0.817	2.105	2.115	0.289	0.290
ω_1 present	0.6541[a]	0.6558[a]	0.6925[a]	0.6927[a]	0.6273[a]	0.6375[a]
Ref. 7			0.7146[a]		0.6892[a]	
ω_2 present	3.1547	3.1529	2.1476	2.1467	3.6167[a]	3.7437[a]
Ref. 7			2.4373		3.9166[a]	
ω_3 present	3.7617[a]	3.8239[a]	3.7493[a]	3.7980[a]	5.0533	5.0536
Ref. 7			3.8724[a]		5.0533	
ω_4 present	9.4357[a]	9.4138[a]	6.4428	6.4182	9.0971[a]	9.7038[a]
Ref. 7			7.3120		9.7108[a]	
ω_5 present	9.4642	9.7942	8.9153[a]	9.1643[a]	12.749	12.904
Ref. 7			9.2135[a]		12.854	
ω_6 present	12.510	12.558	10.738	10.561	15.160	15.166
Ref. 7			12.187		15.160	
ω_7 present	15.774	15.536	11.704	11.603	15.780[a]	17.405[a]
Ref. 7			13.131		16.632[a]	

[a] Bending modes (each frequencey is associated with two modes, corresponding to bending in the $x_1 - x_3$ and $x_2 - x_3$ planes).

Numerical Studies

To test and evaluate the accuracy of the predictions of the continuum models developed, a number of thermoelastic stress analysis and free vibration problems are solved by these models. Comparisons are made with exact solutions based on direct solution of the actual lattice structure. Two problem sets are presented herein. These problems are 1) stress and free vibration analysis of beamlike lattices; and 2) thermoelastic stress and free vibration analysis of a hexahedral double-layered grid. These problems are discussed subsequently.

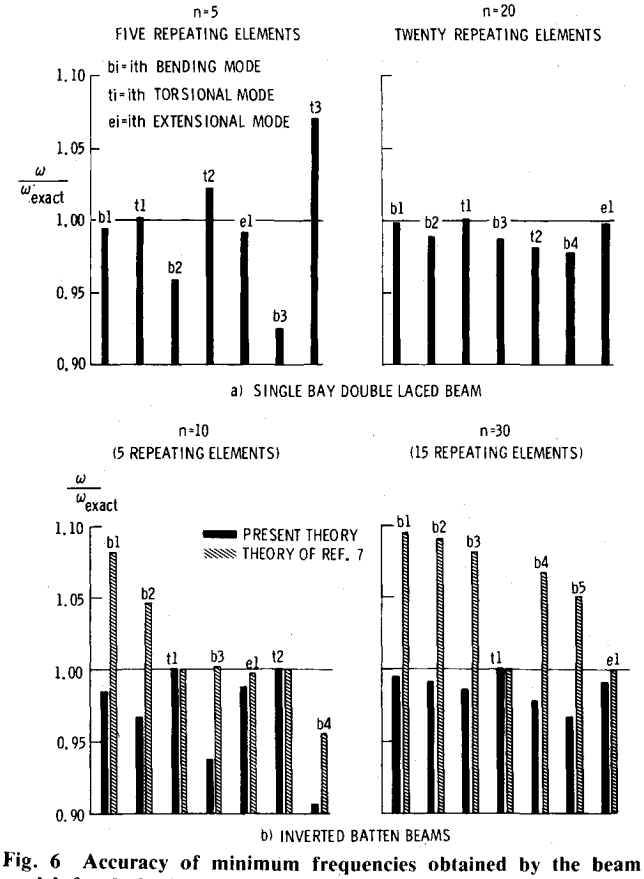

Fig. 6 Accuracy of minimum frequencies obtained by the beam models for the lattices shown in Fig. 1.

Stress and Free Vibration Analysis of Beamlike Lattices

The first problem set considered is that of the stress and free vibration analysis of cantilever beamlike lattices. Three different configurations are considered. The geometric and material characteristics of these structures are shown in Fig. 1. The continuum models for these structures are taken to be cantilever beams having the elastic, thermal, and dynamic coefficients listed in Table 1. For stress analysis problems, the structures were subjected to longitudinal, transverse loadings and twisting moments at their free end. The continuum model solutions presented herein for these problems are closed-form solutions. For the free vibration problems, the continuum beam model solutions are analytic solutions, which are obtained by using the computerized symbolic and algebraic manipulation system MACSYMA.[9] The CPU times required for obtaining the continuum model solutions are so small as to become insignificant in comparison with the CPU times required for the direct solution of the lattice grids. Typical numerical results are shown in Table 3 and Fig. 6.

Table 3 gives the maximum displacements u_1^0 and w^0, rotation ϕ_1 at the free end, and the lowest seven frequencies obtained by the beam models, along with the exact solutions obtained by direct analysis of the actual structure for lattices with 10 bays. The frequencies obtained by the theories of Ref. 7 (with all strain gradients neglected) also are given in Table 3. Figure 6 gives an indication of the accuracy of the lowest seven frequencies obtained by the present theory and theory of Ref. 7 for the single-bay, double-laced and the inverted batten beams. The theory of Ref. 7 was found to overestimate the bending, transverse shear, and torsional stiffnesses of the double-bay, single-laced beams and the bending stiffnesses of the inverted batten beams. Therefore, the minimum frequencies obtained by the theory of Ref. 7 overestimate the frequencies of the actual lattice structure (see Table 3) and do not converge to the exact frequencies as the number of bays increases (see Fig. 6b). On the other hand, the solutions obtained by the present theory are highly accurate, especially when the wavelength of the vibration mode encompasses more than one repeating element. For lattices with 10 bays, the maximum errors in the vibration frequencies were less than 3% and 4% for double-bay, single-laced and single-bay,

Table 4 Comparison of transverse thermal displacement at the center and vibration frequencies (in hertz) obtained by continuum plate models with exact solutions for the double-layered hexahedral grid shown in Fig. 4

	Continuum plate models		
	Refs. 7 and 8	Present	Exact solution
$w_{top} \times 10^2$ (meters)	4.749	5.041	5.077
$w_{bottom} \times 10^2$ (meters)	3.732	4.029	4.064
ω_{11}	4.454	4.481	4.505
ω_{12}	7.573	7.669	7.731
ω_{22}	9.709	9.891	10.082
ω_{13}	10.917	11.161	11.220
ω_{01}	13.094	13.094	12.840
ω_{23}	12.449	12.793	13.062
ω_{14}	14.246	14.726	14.655
ω_{33}	14.630	15.146	15.580
ω_{24}	15.415	16.001	16.178
ω_{15}	17.522	18.319	17.815
ω_{34}	17.174	17.937	18.318

double-laced beams, respectively. For inverted batten beams, the maximum error in the vibration frequencies was 9.3% and reduced to 4.2% when the number of bays was increased to 20. The larger error for the inverted batten beam may be attributed to their complex geometry.

Thermoelastic Stress and Free Vibration Analysis of Platelike Lattice Grid

The second problem set considered is that of the thermoelastic stress and free vibration analysis of the hexahedral double-layered grid. The characteristics of the grid are shown in Fig. 4a. The boundary nodes are restrained in the x_3 direction, as well as along the edge where they lie. The continuum model is taken to be a simply supported square plate having the elastic, thermal, and dynamic coefficients listed in Tables 2 and 3. For thermoelastic stress analysis problems, the temperature is assumed to be uniform at the nodes of the top and bottom surfaces and equal to 100° and 50°C, respectively. The continuum model solutions presented herein are analytic, double-trigonometric series solutions.

Table 4 gives the transverse thermal displacements at the center and the lowest 11 vibration frequencies obtained by the present theory, the theory presented in Refs. 7 and 8, and the exact solutions for the case $n = 8$. The transverse normal strain

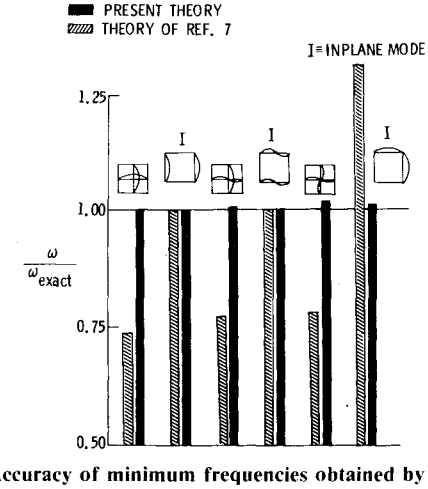

Fig. 7 Accuracy of minimum frequencies obtained by plate models for hexahedral grid shown in Fig. 4a ($A_1/A_2 = 1.6$, $A_d/A_2 = A_v/A_2 = 20$).

ϵ_3^0 was computed using Eq. (22) and is found to be

$$\epsilon_3^0 = \bar{C}_{T33}/\bar{C}_{3333}\, T^0 = \alpha_v T^0 \tag{26}$$

As can be seen from Table 4, the solutions obtained by the present theory are consistently more accurate than those obtained by the theory of Refs. 7 and 8. The maximum errors in the vibration frequencies and transverse thermal displacement obtained by the theory of Refs. 7 and 8 are 7% and 9%, respectively. The corresponding errors in the solutions obtained by the present theory are only 3% and 0.1%. The differences between the predictions of the present theory and those of the theory of Refs. 7 and 8 are due to the differences in the contributions of the vertical and diagonal core members to the elastic and thermal coefficients in the two theories.

In order to amplify the effect of these differences and to serve as a severe test for the accuracy of the two theories, the areas of the core numbers in the grid were increased by two orders of magnitude, and the free vibrations of the new grid were studied. An indication of the accuracy of the lowest six frequencies obtained by the present theory and the theory of Ref. 7 is given in Fig. 7. As can be seen from Fig. 7, even for this extreme case, the present theory is quite accurate. On the other hand, the predictions of the theory of Ref. 7 are considerably in error.

Concluding Remarks

A simple, rational approach is presented for developing continuum models for repetitive beam- and platelike lattices with arbitrary configurations subjected to static, thermal, and dynamic loadings. The continuum models account for the local effects in the repeating element of the actual structures and are characterized by their thermoelastic strain and kinetic energies, from which the equations of motion and constitutive relations can be derived. The procedure for developing the expressions for the thermoelastic strain and kinetic energies is based on introducing kinematic assumptions to reduce the dimensionality of the lattice; expressing the longitudinal strains in the individual members in terms of Taylor series expansions of the strain components in the coordinate directions; and obtaining effective thermoelastic and dynamic coefficients of the continuum in terms of the material properties and geometry of the original lattice structure.

Numerical results are presented for the stress and free vibration analysis of cantilever beamlike lattices and simply supported, double-layered hexahedral grid. These examples demonstrate the high accuracy of the continuum models developed even for lattices with a small number of panels. Moreover, it is shown that, for lattices with large diagonal or core members, inclusion of the local effects in the repeating element in the continuum model is necessary to obtain correct thermoelastic coefficients. If these effects are not included, significant errors can result in the predictions of the continuum models. The real potential of the continuum models developed herein can be realized for lattice structures with a large number of panels where either a small number of finite elements are used for their analysis or, whenever applicable, analytic solutions are obtained.

References

[1] Heki, K., and Saka, T., "Stress Analysis of Lattice Plates as Anisotropic Continuum Plates," *Proceedings of the 1971 IASS Pacific Symposium, Part II on Tension Structures and Space Frames*, Tokyo and Kyoto, Japan, 1972, pp. 663-674.

[2] Kollar, L., "Analysis of Double-Layered Space Trusses with Diagonally Square Mesh by the Continuum Method," *Acta Technica Academiae Scientiarum Hungaricae*, Tomus 76, 1974, pp. 273-294.

[3] Dean, D. L. and Avent, R. R., "State of the Art of Discrete Field Analysis of Space Structures," *Proceedings of the Second International Conference on Space Structures*, edited by W. J. Supple, Univ. of Surrey, Guildford, England, Sept. 1975, pp. 7-16.

[4]Renton, J.D., "The Related Behavior of Plane Grids, Space Grids and Plates," *Space Structures,* Blackwell, Oxford, 1967, pp. 19-32.

[5]Renton, J.D., "General Properties of Space Grides," *International Journal of Mechanical Sciences,* Vol. 12, 1970, pp. 801-810.

[6]Soare, M., "Application of the Equivalent Continuum Method to the Analysis of Double-Layer Parallel Square Mesh Grids, *Buletinul Stiintific al Institutului de Constructii Bucuresti,* Vol. 14, Jan. 1971, pp. 251-269.

[7]Noor, A.K., Greene, W.H., and Anderson, M.S., "Continuum Models for Static and Dynamic Analysis of Repetitive Lattices," *Proceedings of the AIAA/ASME/SAE 18th Structures, Structural Dynamics and Materials Conference,* San Diego, Calif., March 21-23, 1977, pp. 299-310.

[8]Noor, A.K., "Thermal Stress Analysis of Double-Layered Grids," *Journal of the Structural Division, ASCE,* Vol. 104, Feb. 1978, pp. 251-262.

[9]Noor, A.K. and Andersen, C.M., "Computerized Symbolic Manipulation in Structural Mechanics – Progress and Potential," *Proceedings of the Symposium on Future Trends in Computerized Structural Analysis and Synthesis,* Pergamon Press, New York, 1978, pp. 95-118.

From the AIAA Progress in Astronautics and Aeronautics Series..

AERODYNAMIC HEATING AND THERMAL PROTECTION SYSTEMS—v. 59

HEAT TRANSFER AND THERMAL CONTROL SYSTEMS—v. 60

Edited by Leroy S. Fletcher, University of Virginia

The science and technology of heat transfer constitute an established and well-formed discipline. Although one would expect relatively little change in the heat transfer field in view of its apparent maturity, it so happens that new developments are taking place rapidly in certain branches of heat transfer as a result of the demands of rocket and spacecraft design. The established "textbook" theories of radiation, convection, and conduction simply do not encompass the understanding required to deal with the advanced problems raised by rocket and spacecraft conditions. Moreover, research engineers concerned with such problems have discovered that it is necessary to clarify some fundamental processes in the physics of matter and radiation before acceptable technological solutions can be produced. As a result, these advanced topics in heat transfer have been given a new name in order to characterize both the fundamental science involved and the quantitative nature of the investigation. The name is Thermophysics. Any heat transfer engineer who wishes to be able to cope with advanced problems in heat transfer, in radiation, in convection, or in conduction, whether for spacecraft design or for any other technical purpose, must acquire some knowledge of this new field.

Volume 59 and Volume 60 of the Series offer a coordinated series of original papers representing some of the latest developments in the field. In Volume 59, the topics covered are 1) The Aerothermal Environment, particularly aerodynamic heating combined with radiation exchange and chemical reaction; 2) Plume Radiation, with special reference to the emissions characteristic of the jet components; and 3) Thermal Protection Systems, especially for intense heating conditions. Volume 60 is concerned with: 1) Heat Pipes, a widely used but rather intricate means for internal temperature control; 2) Heat Transfer, especially in complex situations; and 3) Thermal Control Systems, a description of sophisticated systems designed to control the flow of heat within a vehicle so as to maintain a specified temperature environment.

Volume 59—432 pp., 6×9, illus. $20.00 Mem. $35.00 List

Volume 60—398 pp., 6×9, illus. $20.00 Mem. $35.00 List

TO ORDER WRITE: Publications Dept., AIAA, 1290 Avenue of the Americas, New York, N.Y. 10019